Critical behavior of a three-dimensional kinetic gelation model

Ashvin Chhabra,* D. Matthews-Morgan,† and D. P. Landau
Center for Simulational Physics, University of Georgia, Athens, Georgia 30602

H. J. Herrmann
Service de Physique Theorique, Centre d'Etudes Nucléaires de Saclay, 91191 Gif-sur-Yvette Cedex, France
(Received 24 February 1986)

We present extensive results from a computer-simulation study of a kinetic growth model for radical-initiated irreversible gelation. Lattices as large as $100\times100\times100$ were used to examine polymerization of a system of tetrafunctional and bifunctional monomers with initiator concentrations c_I, ranging from 3×10^{-2} to 3×10^{-6}. The cluster-size distribution shows unexpected oscillations which become increasingly pronounced as $c_I\to0$. The scaling properties of the cluster-size distribution cannot be described by simple droplet scaling theory, and we propose a generalized form for the scaling. The bulk properties show critical exponents which are independent of c_I and identical to percolation values within the errors. The amplitude ratio C^-/C^+ is not independent of c_I. The backbone of the largest cluster at the gel transition is also investigated and its fractal dimension is found to be distinctly larger than that of a random percolation cluster at p_c.

I. INTRODUCTION

The formation of an infinite macromolecule (gelation) has been investigated theoretically for many years now. The earliest description of this sol-gel transition was provided by Flory[1] and Stockmayer[2] who used a very simple yet effective model involving percolation on a Cayley tree. de Gennes[3] and Stauffer[4] later drew the analogy between gelation and critical-point behavior and suggested that percolation on a real lattice might provide a more realistic description of the sol-gel transition. The qualitative behavior of these models is similar but the critical-point exponents are quite different. More recently, Herrmann, Landau, and Stauffer[5] (HLS) found that a realistic model for addition polymerization (a specific kind of gelation) introduced by Manneville and de Seze[6] seemed to be in a different universality class than percolation. This new universality class, characterized by the same exponents γ and β as percolation but by a different ratio of critical amplitudes, seems to be due to the kinetic nature of this problem as compared to the static description of standard percolation. The relevance of the kinetic aspect for this problem of gelation puts the work that we want to report here into the general context of growth models[7]—a subject of high current interest.

Addition polymerization is the mechanism by which macromolecules are formed through the cross-linking of linearly growing polymers. At some time in the growth process a network of cross-linked chains that spans the whole system might appear. This appearance of an infinite macromolecule (gel) is the phase transition that we want to study in some detail by computer simulations using a model on a lattice.

The individual linearly growing polymer or walk already has interesting kinetic properties that are discussed in recent publications.[8–10] Growing walks and diffusion-limited aggregation[11] (DLA) are the two most-studied one-cluster growth mechanisms and the best easy-to-define models showing the essential nontrivial features of growth. The study of the attaching of many clusters aggregating after diffusion,[12–14] i.e., the many-cluster version of DLA, yields interesting behavior in the cluster-size distribution[15] and seems to explain some coagulation phenomena of the type of polycondensation but shows an infinite gel time.[14] In a similar spirit, addition polymerization as described in this paper is the many-cluster version of some kinetic growth walks.[7]

In the next section we shall describe the model and simulation method as well as the theoretical foundation for the analyses used. Section III contains results and discussions and in Sec. IV we present our conclusions.

II. BACKGROUND

A. Model

The model which we have studied is almost identical to that used by HLS and was described in Ref. 5. Monomers are placed randomly on the sites of an $L\times L\times L$ simple-cubic lattice whose opposite faces are connected by periodic boundary conditions. These monomers may be tetrafunctional with concentration c_t, bifunctional with concentration c_b, or zero functional (solvent) with concentration c_s. The concentrations must obey the constraint

$$c_t+c_b+c_s=1\ . \tag{1}$$

A number n_I of initiators are also placed randomly on the lattice. Historically, the concentrations of initiators c_I has been given in terms of the number of possible bonds in the system, and hence $n_I=3c_IL^3$. These initiators bind to a monomer thus reducing the monomer functionality by one. The initiators saturate, opening up a double bond within the monomer on that site, leaving a radical. Sites

having a radical are called active centers and they can then bond to a nearest neighbor.

B. Simulation method

We have used a technique which begins by randomly choosing an active center. We then pick a nearest-neighbor site to this active center and attempt to form a bond between them. If this nearest-neighbor site is already fully bonded, we choose another active center and repeat the process. If the nearest-neighbor site is not already fully bonded, the active center jumps to this site forming a bond in the process. If two active centers bond together, they annihilate; when all of the nearest neighbors (of an active center) are fully bonded the active center is "trapped."[16] Growth is described schematically in Fig. 1.

After a predetermined number of bonds have been formed, we calculate various properties; the chemical conversion factor p, defined as the number of bonds grown divided by the maximum possible number $3L^3$, specifies the degree of polymerization. We determine the normalized number of clusters n_s of size s (i.e., the number of clusters of size s divided by the total number of sites in the lattice), the "susceptibility" or average molecular weight

$$\chi=\sum_s s^2 n_s \ , \tag{2}$$

and the "gel fraction"

$$G=1-\sum_s s n_s \ , \tag{3}$$

where the sums exclude the largest cluster. This entire procedure is repeated many times using different random numbers to produce different growth samples, and then averages are calculated over all the samples. In an infinite system G is zero for all p up to the gel point p_c; for $p>p_c$ the gel fraction grows as

$$G=B^+\left[\frac{p-p_c}{p_c}\right]^{\beta} . \tag{4}$$

In the vicinity of p_c the susceptibility also shows critical behavior of the form

$$\chi p=C^-/\!\!\not{\epsilon}^{-\gamma} \ , \quad p<p_c \ , \tag{5a}$$

$$=C^+/\!\!\not{\epsilon}'^{-\gamma} \ , \quad p>p_c \ , \tag{5b}$$

where $/\!\!\not{\epsilon}=(p_c-p)/p$, $/\!\!\not{\epsilon}'=(p-p_c)/p_c$, C^- is the critical amplitude below p_c, and C^+ is the amplitude above p_c. The correlation length ξ diverges at p_c as

$$\xi=\xi_0\left|\frac{p-p_c}{p_c}\right|^{-\nu} \tag{6}$$

and at p_c the infinite cluster is a fractal object. The fractal dimension of the cluster may be determined from the relation

$$S=R^{d_f} \ , \tag{7}$$

where S is the mass of the largest cluster which is within a radius R of a point on the cluster.

C. Finite-size scaling

Data obtained for finite lattices can be related to the corresponding infinite lattice singularities through the use of finite-size-scaling theory. This approach, first developed for thermal phase transitions,[17] expresses bulk quantities of $L\times L\times L$ systems in terms of homogeneous scaling functions of a variable $x=/\!\!\not{\epsilon}L^{1/\nu}$ or $x=/\!\!\not{\epsilon}'L^{1/\nu}$. For the gel fraction the appropriate form is

$$G=L^{-\beta/\nu}\mathcal{G}(x) \ , \tag{8}$$

where $\mathcal{G}(x)$ is a scaling function. For the susceptibility the form which we use is

$$\chi p=L^{\gamma/\nu}\mathcal{F}(x) \ . \tag{9}$$

This scaling is valid asymptotically for large L. Thus by making double logarithmic plots of $GL^{\beta/\nu}$ versus x and $\chi pL^{-\gamma/\nu}$ versus x, we can vary p_c and the critical exponents until the data collapse onto single curves (one curve for $p<p_c$ and one for $p>p_c$) defining $\mathcal{F}(x)$ and $\mathcal{G}(x)$. In addition, the behavior of Eqs. (8) and (9) must correctly reproduce the infinite lattice critical behavior in the limit that $L\to\infty$. This restriction then requires that

$$\mathcal{G}(x)\to x^{\beta} \ , \quad x\to\infty \ , \quad p>p_c \tag{10a}$$

$$\mathcal{F}(x)\to x^{-\gamma} \ , \quad x\to\infty \tag{10b}$$

and the scaling plots must obey this restriction as a consistency check. For a description of what happens to $\mathcal{G}(x)$ as $x\to\infty$ and $p<p_c$ see Ref. 18.

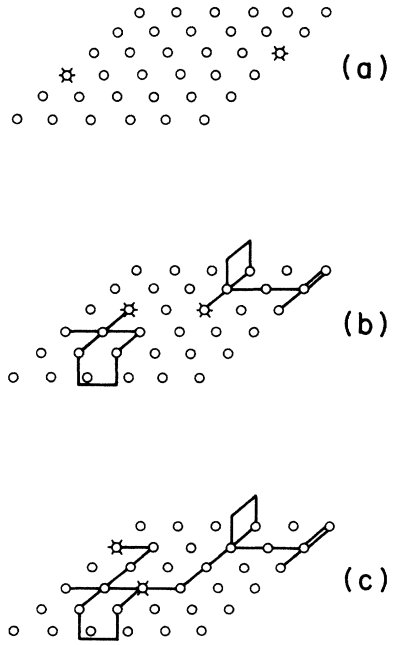

FIG. 1. Schematic view of growth within a single layer: (a) initial lattice with two initiators shown by (○); (b) lattice showing bonds formed after growth has taken place (including bonds to one layer above and one layer below) with active centers shown by (☆); (c) lattice after growth has joined the clusters produced by the two initiators.

D. Droplet scaling theory

As bonds are formed in the system a distribution of clusters results in which each cluster is composed of the collection of sites which are connected to each other at least once by an unbroken string of bonds. This situation is similar to that which occurs for thermal transitions where "droplets" of ordered material form. The bulk properties for these transitions have been described in terms of a droplet theory proposed by Essam and Fisher[19] and used by Stauffer[4] to analyze random percolation. In terms of our variables the cluster-size distribution $n_s(p)$, which gives the number of clusters of size s, should have the following behavior near p_c:

$$n_s(p)=s^{-\tau}f(|p-p_c|s^{\sigma}) . \tag{11}$$

The moments of this distribution can also be related to bulk properties. For example, the second moment of $n_s(p)$ yields the critical behavior of the susceptibility through

$$\chi=\sum_s s^2 n_s \sim C^{\mp}|(1-p/p_c)|^{-\gamma} , \tag{12}$$

and thus by substituting Eq. (11) into (12) one can show

$$\gamma=\frac{3-\tau}{\sigma} .$$

The ratio of critical amplitudes C^- for $p<p_c$ and C^+ for $p>p_c$ is defined as $R=C^-/C^+$.

E. Backbone

The backbone[20] of a random structure is an important concept to the understanding of its dynamical properties such as the electrical conductivity[3,21] or the elasticity.[22] The definition of the backbone depends on the end points (or bars) between which it is chosen. Suppose we choose two points P_1 and P_2 on the largest cluster separated by a distance comparable to the correlation length ξ. If we put an electrical potential drop from P_1 to P_2 and treat the bonds as conductors, then the set of current-carrying bonds is called the backbone and the remaining bonds are called dangling ends. In Fig. 2 we show the backbone as thick lines and the dangling ends as thin lines. An equivalent definition of the backbone is to consider it as the intersection of all the self-avoiding walks between P_1 and P_2.

A random fractal object, like a percolation cluster at p_c, has a backbone which is also a fractal and its fractal dimension d_f^{BB} is defined through

$$S_{BB}\sim L^{d_f^{BB}} \tag{13}$$

with S_{BB} being the number of sites of the backbone inside a box of length L. d_f^{BB} is, in general, smaller than the fractal dimension d_f^{LC} of the original cluster. The exponent d_f^{BB} has turned out to be universal like other critical exponents, but up to now it has not been possible to establish any relationship between d_f^{BB} and any other known critical exponent. Thus presently, d_f^{BB} is considered to be a completely independent exponent that describes the internal structure of the cluster.[23] In terms of the voltage distribution over the cluster after application of an external potential, d_f^{BB} describes the scaling of the zeroth moment (i.e., the mass of the backbone) and is the first of a whole hierarchy of fractal dimensions.[24]

Another interesting notion that has been recently introduced is the "elastic backbone."[25] It is based on the concept that elasticity in the linear regime can be described by small springs which sit only in the bonds of a cluster and are free to pivot about connection points. In this case, it is difficult to imagine that more than just the shortest paths connecting the points P_1 and P_2, at which the force is applied, should contribute to this elasticity, because any strand longer than the shortest path will not even be stretched out at infinitesimally small strain. So the elastic backbone is defined as being all the sites of the cluster that lie on the union of all the shortest paths between the points P_1 and P_2. The elastic backbone is a subset of the backbone and is marked in Fig. 2 as the jagged lines. The elastic backbone is, in general, a fractal with a fractal dimension d_f^{EB}, and also in this case no relation is known between d_f^{EB} and other usual critical exponents.

Technically, the backbone and the elastic backbone are obtained by the burning algorithm described in Ref. 25. The points P_1 and P_2 are chosen to be the two closest points to diagonally opposite corners of the cube in which the simulation took place. Furthermore, the sums of the x, y, and z components of the displacements of P_1 and P_2 from their respective corners must each be smaller than L. If this is not the case, the backbone is discarded.

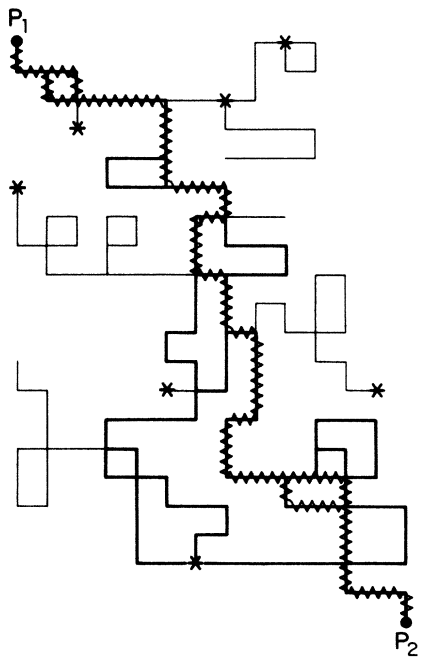

FIG. 2. Schematic representation of the largest cluster (——), backbone (—), and elastic backbone (∿∿). End points are P_1 and P_2 and active centers are shown by *.

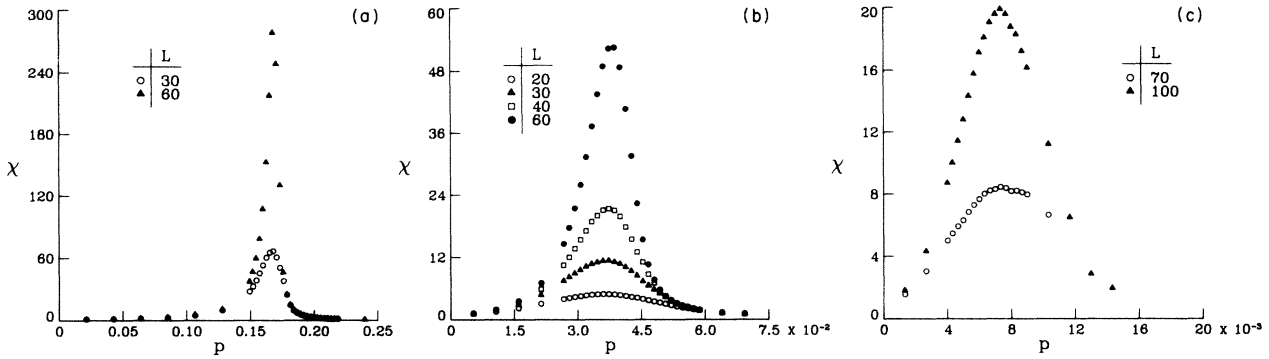

FIG. 3. Susceptibility (second moment of the cluster-size distribution) χ as a function of p for three different values of c_I: (a) $c_I=3\times10^{-2}$, (b) $c_I=3\times10^{-4}$, (c) $c_I=3\times10^{-6}$.

III. RESULTS AND DISCUSSION

A. Bulk properties

In earlier studies[5,16] we reported results for models with solvent and/or bifunctional units. In this paper we concentrate primarily on tetrafunctional units allowing a wide variation of c_I and, in addition, have obtained many more growth samples than were used in this earlier work.

The susceptibility and gel fraction data show the same qualitative behavior over the entire range of c_I which was investigated. In Fig 3 we show data for the susceptibility for three values of c_I. The maxima in all cases are depressed strongly for the smaller lattices, and this finite-size rounding becomes particularly important as $c_I\to0$. The critical behavior can be extracted using finite-size-scaling theory described earlier in Sec. II C. Finite-size-scaling plots for the susceptibility for these data are shown in Fig. 4. The critical exponents determined from these (and similar plots for other values of c_I) were essentially identical in all cases: $\gamma=1.80\pm0.10$ and $\nu=0.82\pm0.07$ as compared with $\gamma=1.78\pm0.06$ and $\nu=0.88\pm0.02$ for percolation.[26] For very small lattices the simple finite-size-scaling expressions were not adequate since correction terms became important. Thus for $c_I=3\times10^{-2}$ we could not use data for $L<20$; the finite-size effects become increasingly important with decreasing lattice size so that for $c_I=3\times10^{-6}$ the correction terms are significant even for $L=60$. (It is perhaps worth remarking that substantially larger lattices are required than are needed to study finite-size behavior in simple models with thermal phase transitions, such as Ising or Potts models. One can understand this effect since the typical distance between initiators is $\propto c_I^{-1/3}$, i.e., increases with decreasing c_I, which would suggest that one needs an L some 20 times larger for $c_I=3\times10^{-6}$ than for $c_I=3\times10^{-2}$ to have equivalent size effects.

Finite-size-scaling plots for the gel fraction are shown in Fig. 5. Corrections to scaling are quite important in the gel phase but are of less importance for $p<p_c$. Our best estimates for the critical exponents are $\beta=0.40\pm0.05$ and $\nu=0.8\pm0.1$, whereas $\beta=0.44\pm0.01$ for percolation.[26] This estimate for ν agrees quite well with that obtained from the analysis of χ.

From these finite-size-scaling plots we can extract critical amplitudes as well as exponents, and these are plotted in Fig. 6. Also of interest is the amplitude ratio $R=C^-/C^+$, which according to standard scaling assumptions should be a universal quantity for percolation-like critical behavior. This is strengthened for percolation by the field-theoretical work of Aharony.[27] In $d=3$ one finds $R\approx10$, and in mean-field theory $R=1$, for percolation. As we show in Fig. 6, the ratio C^-/C^+ is not universal but varies as $\sim c_I^{0.18}$ over four decades in c_I. This relation implies that $R\to0$ as $c_I\to0$. This result would seem rather unphysical and we have also explored

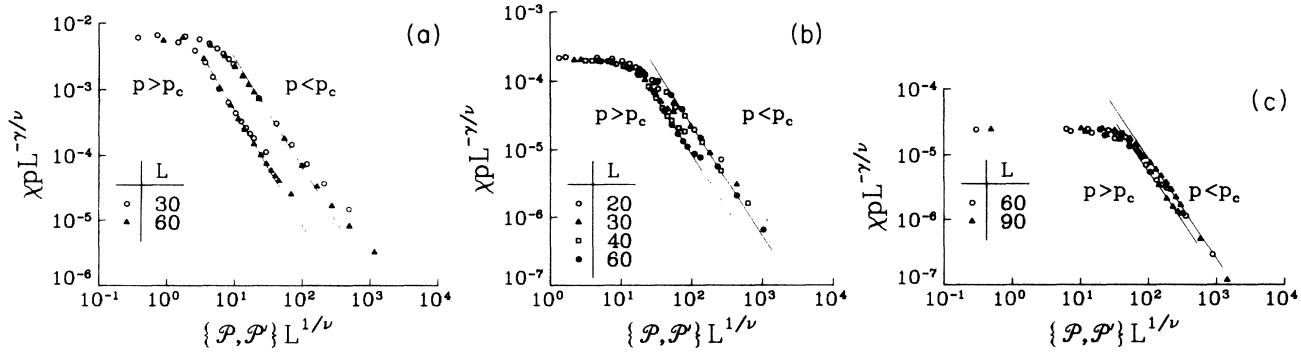

FIG. 4. Finite-size-scaling plots for the susceptibility χ: (a) $c_I=3\times10^{-2}$, $p_c=0.16975$, $\gamma=1.75$, $\nu=0.8$; (b) $c_I=3\times10^{-4}$, $p_c=0.0385$, $\gamma=1.80$, $\nu=0.8$; (c) $c_I=3\times10^{-5}$, $p_c=0.0167$, $\gamma=1.85$, $\nu=0.8$.

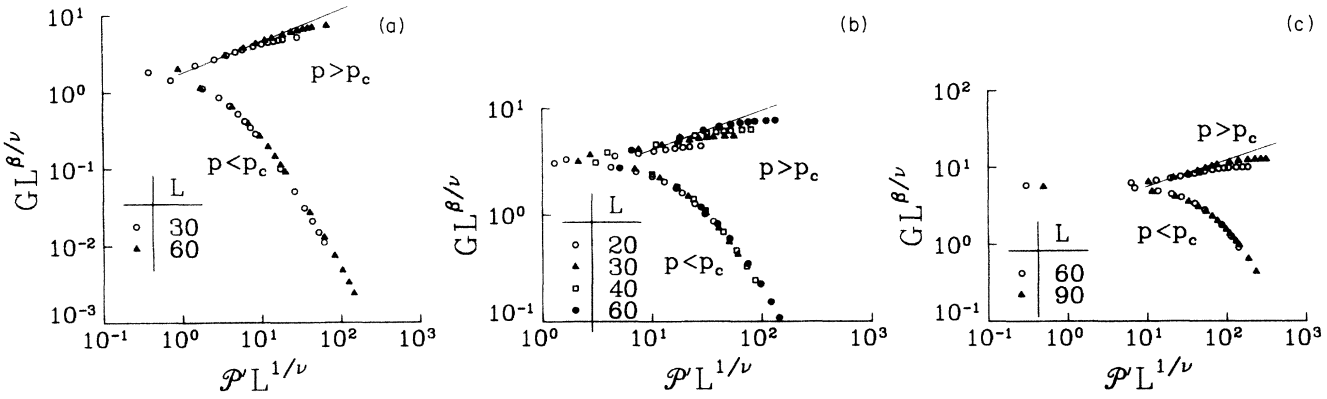

FIG. 5. Finite-size-scaling plots for the gel fraction G: (a) $c_I=3\times10^{-2}$, $p_c=0.16975$, $\beta=0.40$, $\nu=0.8$; (b) $c_I=3\times10^{-4}$, $p_c=0.0385$, $\beta=0.40$, $\nu=0.8$; (c) $c_I=3\times10^{-5}$, $p_c=0.0167$, $\beta=0.45$, $\nu=0.8$.

the possibility that $R\rightarrow$const as $c_I\rightarrow0$. In Fig. 6 we show the variation of $R-1$ with c_I ($R=1$ is the totally symmetric case). This behavior is also consistent with a power law but the power is dependent on the actual value to which R tends as $c_I\rightarrow0$. The variation of the critical value of the conversion factor p_c at the gel point is also shown as a function of c_I in Fig. 6. From this plot, we deduce that $p_c\propto c_I^{\phi}$ with $\phi\simeq\frac{1}{3}$. This number can be understood through the effective fractal dimension of the individual walks in the following way: p_c is reached when the individual walks first touch each other, i.e., when each walk covers a volume $\propto c_I^{-1}$. If D_f is the fractal dimension of a walk, this implies the relation

$$p_c\propto c_I^{1-D_f/d}. \tag{14}$$

It has been numerically demonstrated[10] that grown self-avoiding walks of moderate length—and this is essentially what our individual walks are—have an effective dimension of 2 in $d=3$. This effective value leads to the exponent ϕ which we found [see Eq. (14)]. We also show the individual amplitudes C^- and C^+ as a function of c_I in Fig. 6.

B. Cluster-size distribution

Unlike the monotonic behavior observed for percolation,[28] the cluster-size distribution n_s shows quite striking oscillatory behavior as a function of s. This behavior is different from that observed by other authors.[6,29] (We have reported our preliminary findings elsewhere.[30]) Typical data for n_s at p_c are shown for different values of c_I in Fig. 7. In all cases a pronounced peak is seen at a "characteristic size" s^* and succeeding peaks are located at integer multiples of s^*. This behavior is found for $p<p_c$ and $p>p_c$ as well as shown in Fig. 8. We believe that the peak at s^* is composed of clusters which have been produced by a single initiator and the clusters at ms^* (where m is an integer) correspond to those produced by the merging of m chains, each of mean size s^*. Since all active centers allow growth to begin at time $t=0$, the resultant clusters are thus all about the same size (excluding those which involve trapped or annihilated active centers) at some later time t. Conversely, if active centers are continuously created in time,[31] no oscillations are seen. The data also clearly show that the oscillations become increasingly pronounced as $c_I\rightarrow0$. For large values of s the data show a strong dependence on lattice size, and for small values of L can show a spurious increase at large s (see Fig. 9). This behavior was also seen by Donoghue and Gibbs[32] who reformulated Flory-Stockmayer theory to explicitly predict the entire cluster-size distribution in a model system of finite size rather than simply use the "most probable" distribution in the limit that $L\rightarrow\infty$.

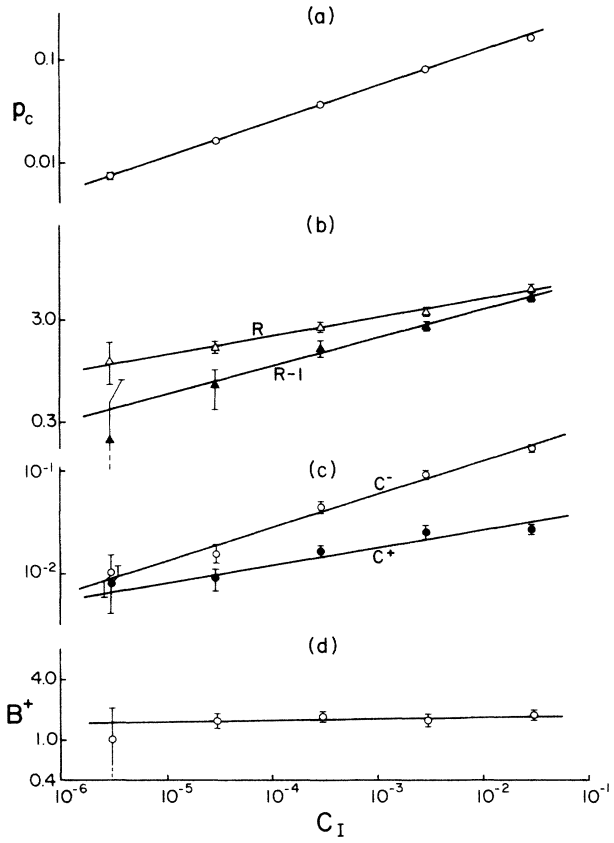

FIG. 6. Dependence of critical parameters on c_I: (a) p_c; (b) R and $(R-1)$; (c) C^- and C^+; (d) B^+.

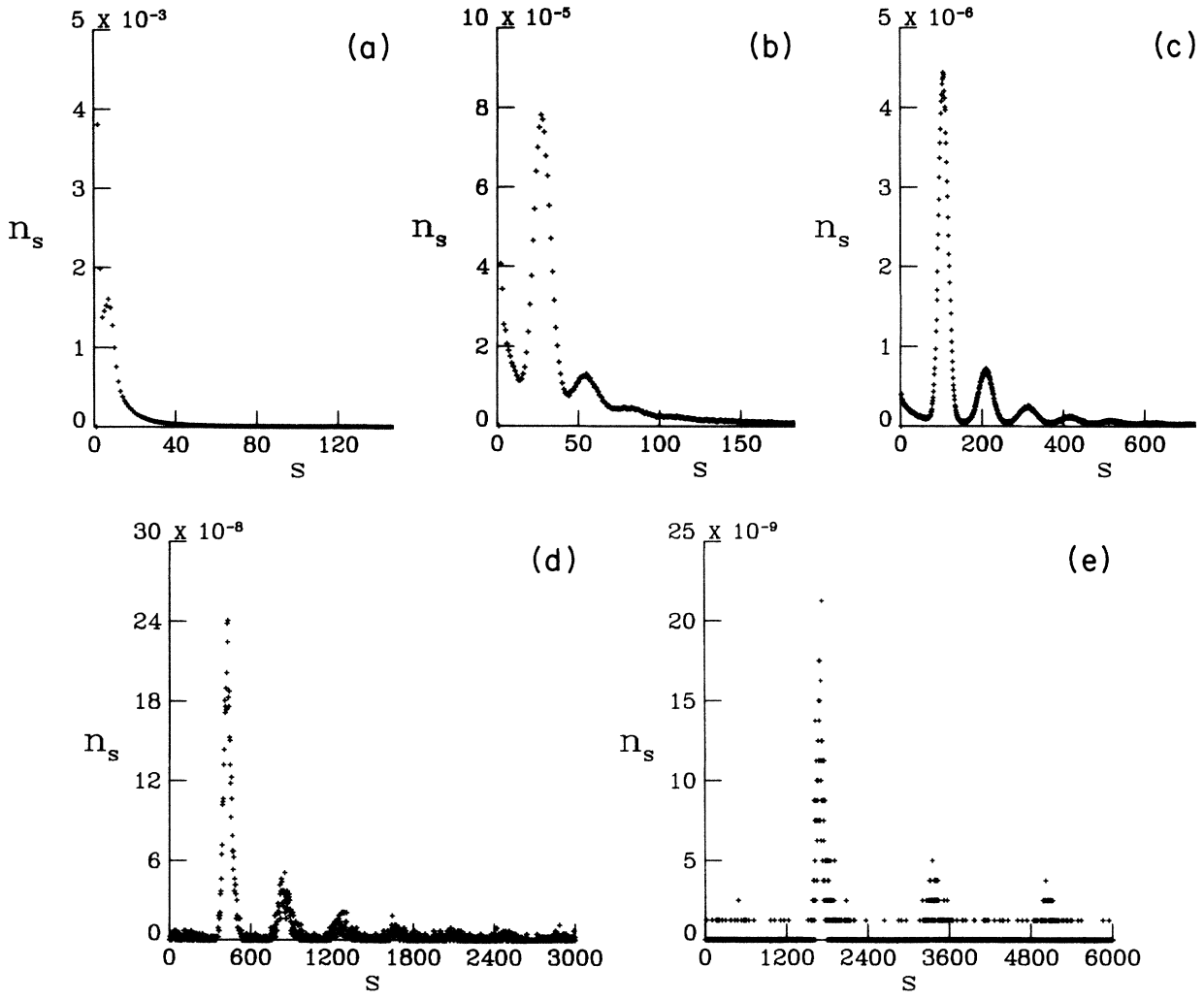

FIG. 7. Cluster-size distribution n_s at p_c for different c_I: (a) 3×10^{-2}, $L=60$; (b) 3×10^{-3}, $L=60$; (c) 3×10^{-4}, $L=60$; (d) 3×10^{-5}; (e) 3×10^{-6}, $L=100$.

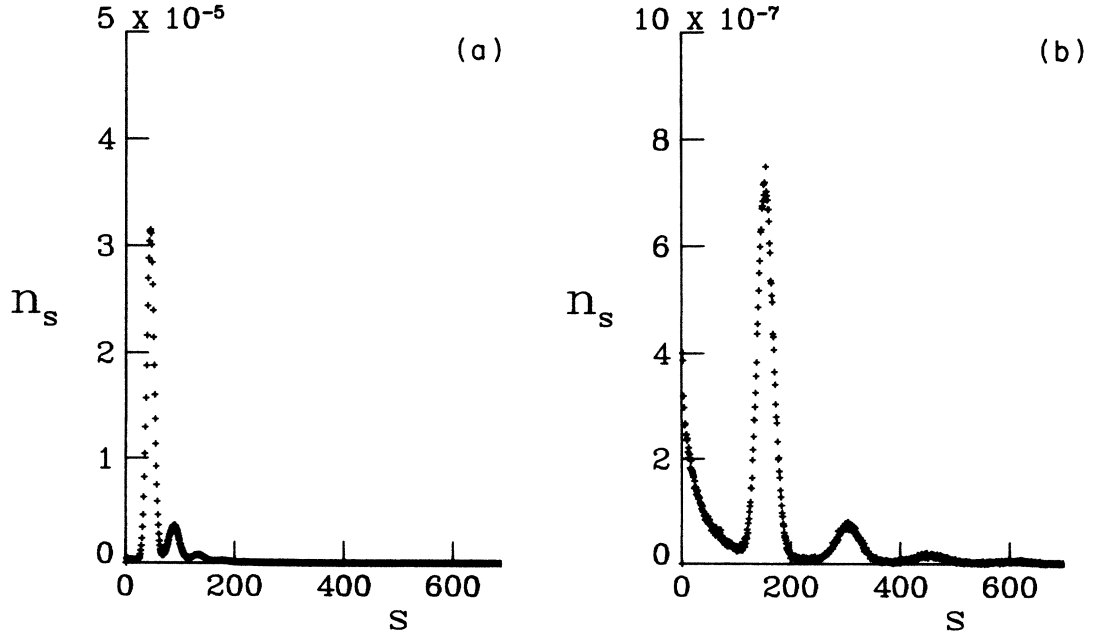

FIG. 8. Cluster-size distribution for $c_I=3\times10^{-4}$: (a) $p=0.016$; (b) $p=0.053$.

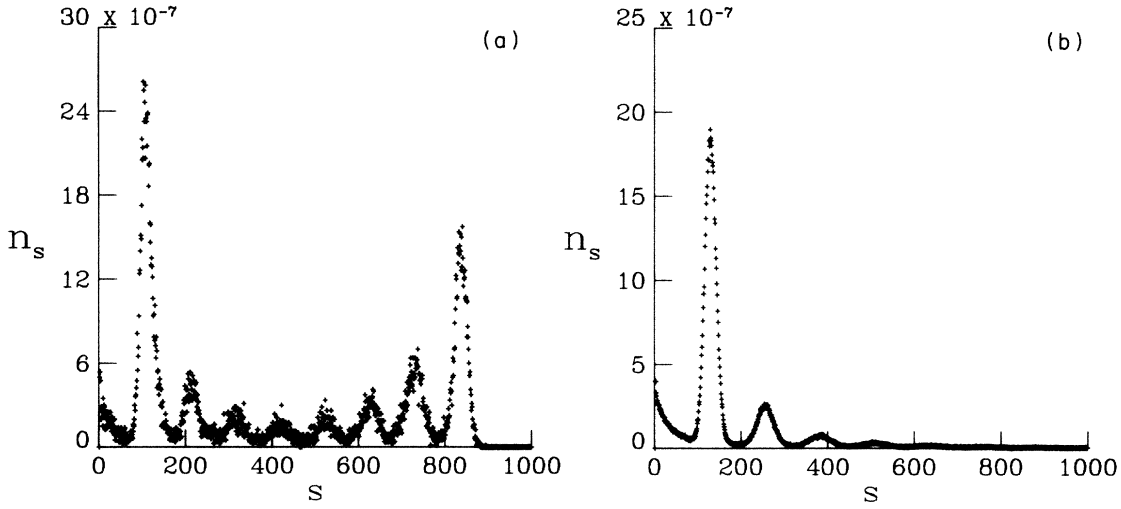

FIG. 9. Effects of finite lattice size on n_s for $p > p_c$ and $c_I = 3 \times 10^{-4}$: (a) data for $L = 20$; (b) data for $L = 60$.

(They did not see oscillations, of course, but their result looked qualitatively like the envelope to the series of maxima seen in Fig. 9.) The cluster-size distributions shown in Fig. 7 appear to have small maxima at $s = 1$ and then to decrease before showing the first large peak at s^*. This is an effect due to annihilation and disappears, as shown in Fig. 10, when we remove the mechanism which destroys active centers when they bond. If the concentration of bifunctional units is greater than zero, the oscillations in the cluster-size distribution are reduced as shown in Fig. 11. According to the droplet scaling form that is valid for percolation, described in Sec. II D, the cluster-size distribution should fall off as $s^{-\tau}$ at the gel point. In Fig. 12, we show a log-log plot of n_s versus s at p_c for $c_I = 3 \times 10^{-4}$. On this scale, the oscillations at ms^* are clearly visible even for "large" m. The envelope of the maxima decays approximately as $s^{-2.5}$ whereas the envelope of the minima does not show a simple power-law decay. The variation of successive minima and maxima suggests that the oscillations persist out to $m = \infty$. The variation of s^* with p is linear (see Fig. 13) and the coefficient increases with c_I. Attempts to scale the cluster-size distribution using the droplet form [Eq. (11)] were unsuccessful. A typical such scaling plot is shown in Fig. 14(a). Instead, we found that relatively good scaling very close to p_c [see Fig. 14(b)] could be obtained using (s/s^*) as the scaling variable and a scaling equation

$$n_s = \left[\frac{s}{s^*}\right]^{-\tau} f(s/s^*) \, . \tag{15}$$

Since $s^* \propto p$, we can equally well use $f(s/p)$. Unfortunately, this form, when combined with Eqs. (2) and (3), does not yield the observed critical behavior since it has no dependence on p_c. If instead we modify the scaling expression to have the form

$$n_s = \left[\frac{s}{p}\right]^{-\tau} \exp[B \, | p - p_c | \, (s/p)^{\sigma} + A \, | p - p_c | \,] f(s/p) \tag{16}$$

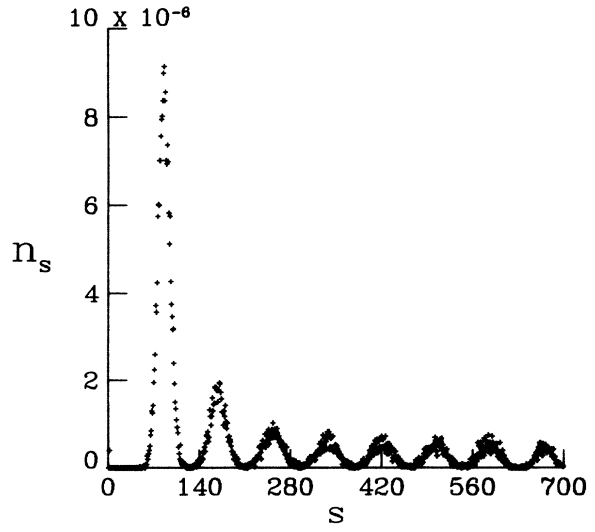

FIG. 10. Cluster-size distribution at p_c with annihilation removed for $c_I = 3 \times 10^{-4}$, $L = 20$.

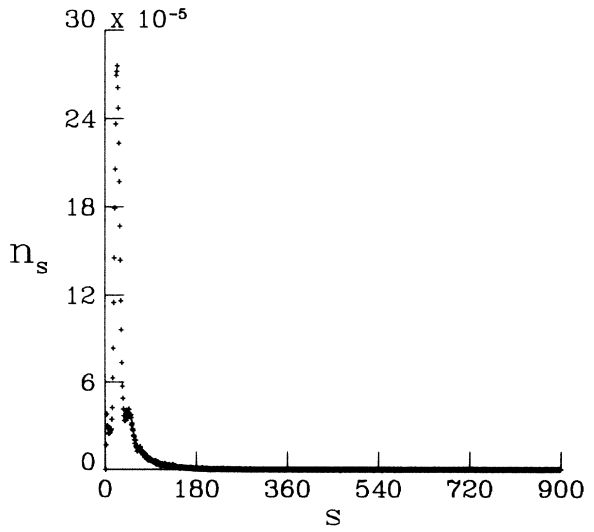

FIG. 11. Cluster-size distribution at p_c for $c_2 = 0.6$, $c_4 = 0.4$, with $c_I = 3 \times 10^{-3}$.

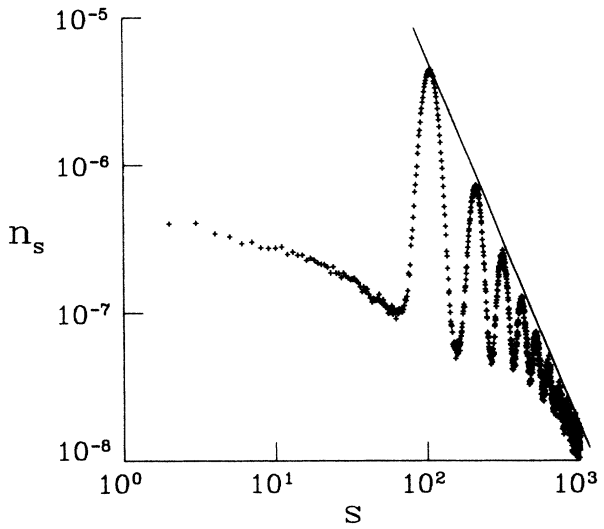

FIG. 12. Cluster-size distribution at p_c for $c_I = 3\times10^{-4}$. The solid line is the envelope to the maxima and has slope 2.48.

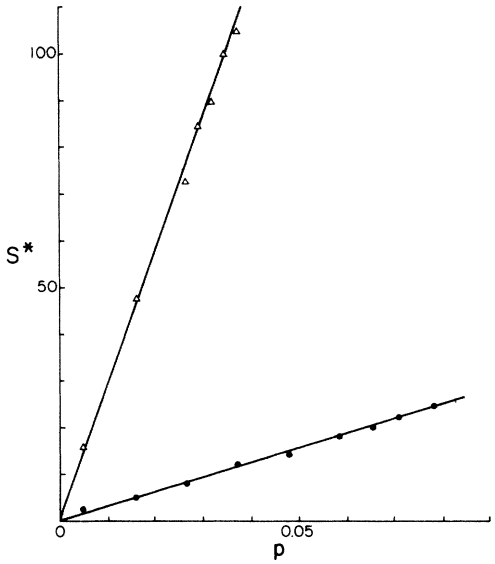

FIG. 13. Variation of s^* with p: $c_I = 3\times10^{-3}$ (●); $c_I = 3\times10^{-4}$ (△).

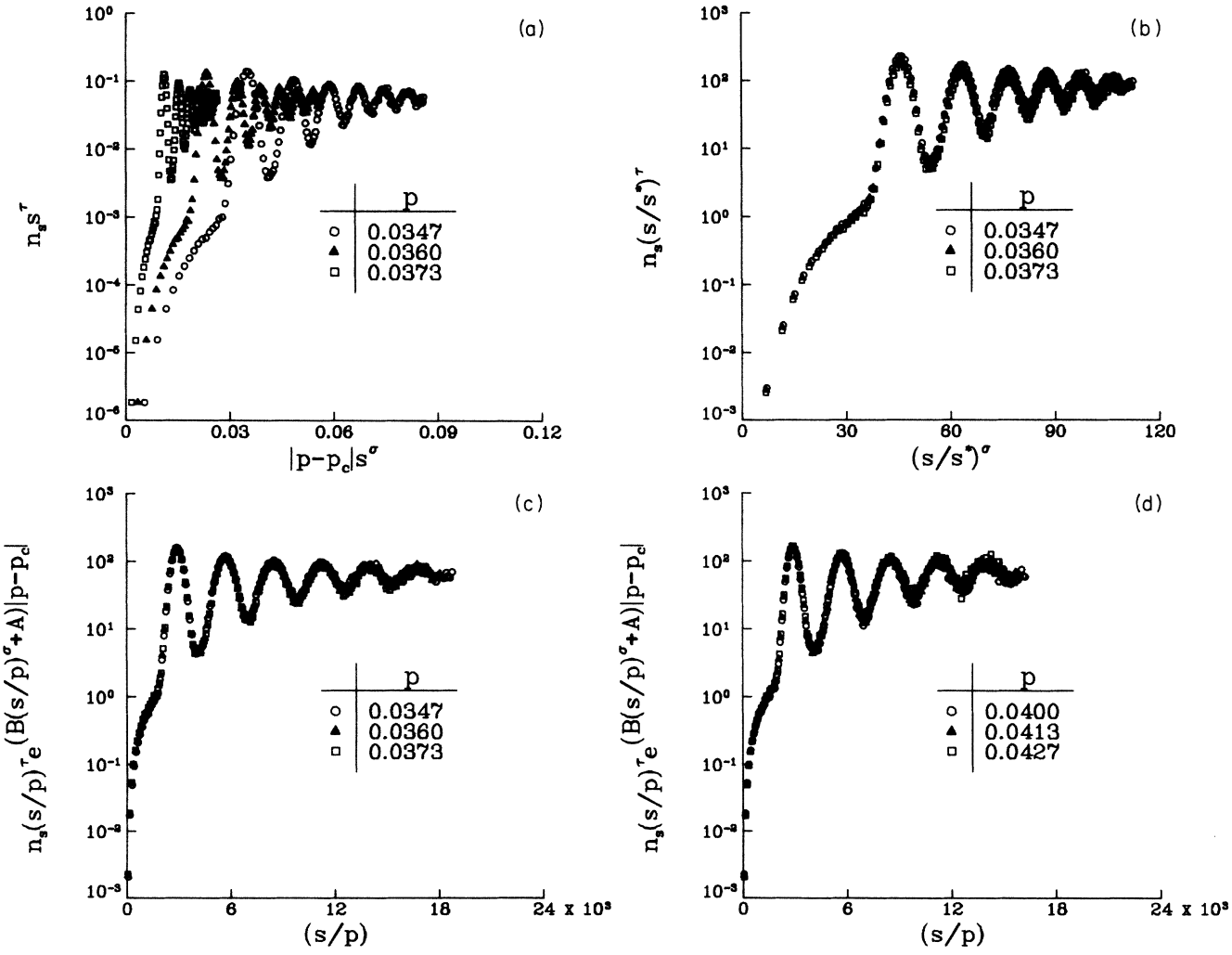

FIG. 14. Scaling plots for the cluster-size distribution with $c_I = 3\times10^{-4}$, $p_c = 0.0385$, $\tau = 2.2$, $\sigma = 0.48$: (a) droplet scaling for $p < p_c$; (b) normalization by s/s^* for $p < p_c$; (c) modified scaling for $p < p_c$. $A = -100$, $B = 0.1$; (d) modified scaling for $p > p_c$ with $A = 0$, $B = 2.6$.

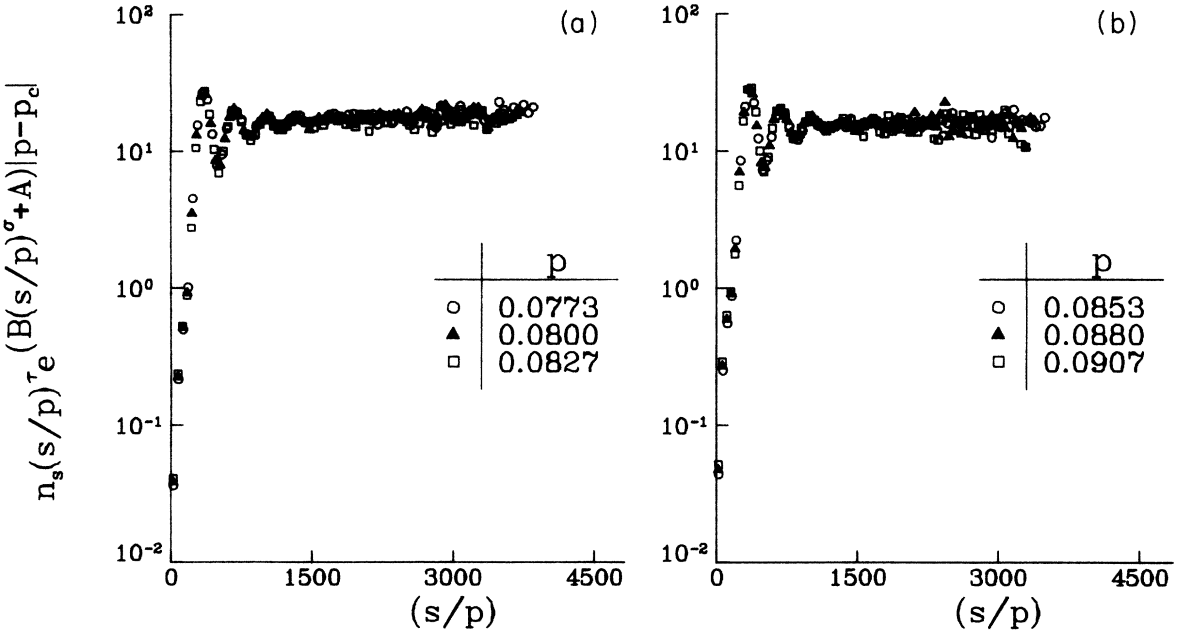

FIG. 15. Modified scaling plots for the cluster-size distribution with $c_I=3\times10^{-3}$, $p_c=0.0845$, $\tau=2.2$, $\sigma=0.48$: (a) $p<p_c$, $A=-50$, $B=0.1$; (b) $p>p_c$, $A=50$, $B=1.0$.

we not only improve the scaling but also reproduce the correct critical behavior [see Fig. 14(c)]. τ and σ are universal exponents, A and B nonuniversal constants. The scaling form is valid for $p>p_c$ as well as for $p<p_c$, only with different values for A and B. In Fig. 15 we show scaling plots, using the modified form of Eq. (16), for $c_I=3\times10^{-3}$. The same general features are observed but with less-pronounced oscillations.

Experiments which could determine the cluster-size distribution in real gels are quite tedious and have thus been performed only rarely. The only accurate study that we are aware of was carried out by Leibler and Schosseler,[33] who studied gelation of polystyrene chains in solution cross-linked by γ-ray irradiation. Unfortunately, this process is not radical initiated growth and the results are not relevant to the simulation data.

C. Backbone properties

For "small" c_I finite-size effects are important for small L, and for "large" c_I the gel clusters are poorly formed for large L so the statistics become poor. The best results over the widest range of L were obtained for $c_I=3\times10^{-4}$. The results for a variety of cluster properties for $c_I=3\times10^{-4}$ are shown in Table I. The values which we obtain for the fractal dimensionality of the largest cluster d_f^{LC} and of the elastic backbone d_f^{EB} are essentially the same as for random percolation in three dimensions. The fractal dimension for the backbone is substantially larger than for percolation and is only slightly smaller than d_f^{LC}.

An interesting question to ask about the structure of a cluster is if it has many loops or if it is essentially treelike. For percolation this has been done by studying the number of loops of the largest cluster L_{LC}, the backbone L_{BB}, and of the elastic backbone L_{EB} as the lattice increases in size.[25] It was found for percolation that these quantities have an exponent relation with an exponent which, within the error bars, is equal to the fractal dimension of the corresponding object. This means that loops are relevant on all length scales. The same analysis has been performed here for kinetic gelation with $c_I=3\times10^{-4}$ and the same result, shown in Fig. 16 and Table I, was found: for the largest cluster, backbone, and elastic backbone the number of loops is, within the error bars, proportional to the mass.

The burning times of the largest cluster T_{LC} and of the backbone T_{BB} are the maximum chemical distances one can find between P_1 and a point on the largest cluster or

TABLE I. Exponents showing the scaling of fundamental cluster properties with system size.

Quantity	Kinetic gelation	Percolation
S_{LC}	2.34±0.12	2.53±0.02[a]
S_{BB}	2.22±0.10	1.74±0.04[b]
S_{EB}	1.47±0.08	1.37±0.07[c]
L_{LC}	2.42±0.10	2.44±0.08[c]
L_{BB}	2.31±0.14	1.87±0.07[c]
L_{EB}	1.52±0.15	1.42±0.05[c]
T_{LC}	1.40±0.15	
T_{BB}	1.44±0.15	
l_p	1.44±0.15	1.33±0.07[c]
N_{LC}^B	1.00±0.10	
N_{BB}^B	1.05±0.10	

[a]Reference 26.
[b]Reference 29.
[c]Reference 25.

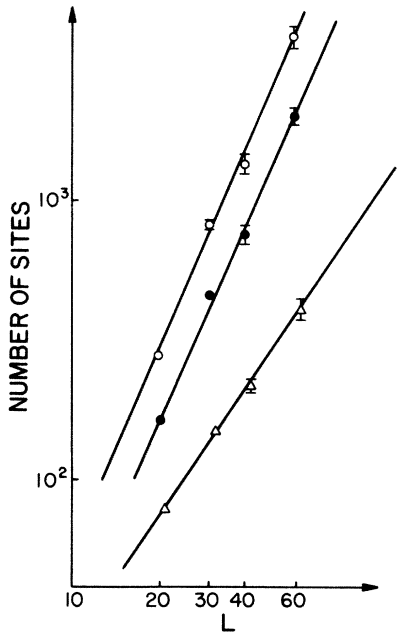

FIG. 16. Finite-size behavior at p_c of the gel cluster (○), backbone (●), and elastic backbone (△) for $c_I = 3\times10^{-4}$.

the backbone, respectively. The length of the shortest path l_p is the chemical distance between P_1 and P_2. All these quantities scale with the same exponent $d_{\min}$ if one increases L as shown in Table I. This exponent $d_{\min}$ is slightly larger than that found for percolation,[25,34] but by an amount which is within the error bars.[35] The fact that $T_{\rm LC}$, $T_{\rm BB}$, and l_p are proportional to each other shows that the clusters are homogeneous in chemical metric. By this, we mean that if one chooses all pairs of points on the cluster of a given Euclidean distance r, their average chemical distances will be a self-averaging quantity and their distribution will become more peaked as larger r is chosen. Finally, in Table I we also show that the maximum number of sites having equal chemical distances from P_1 for the largest cluster $N^B_{\rm LC}$ and for the backbone $N^B_{\rm BB}$ scales with the box size L with an exponent $d_\perp$ of the order 1. This allows us to propose that within the error bars the relation

$$d_f = d_{\min} + d_\perp \tag{17}$$

is valid.

In Fig. 17 we show the size dependence of the largest cluster and the backbone for $c_I = 3\times10^{-3}$ and 3×10^{-5}. For the reasons mentioned earlier, these data are not as complete or of as high quality as for $c_I = 3\times10^{-4}$. The essential features are unchanged; however, $d_f^{\rm LC}$ is the same as for percolation, with our error estimates, and $d_f^{\rm BB}$ is 5–10% smaller than $d_f^{\rm LC}$ and substantially larger than for percolation.[36] (There is a very small systematic variation with c_I, but this is well within the limits of our errors and we believe it is not significant.)

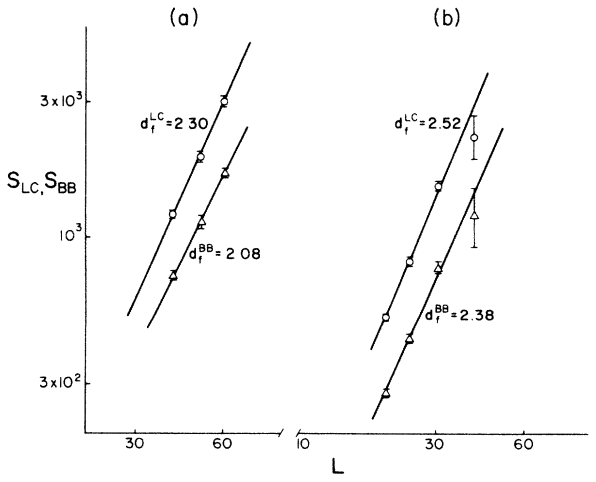

FIG. 17. Finite-size behavior at p_c of the gel cluster and the backbone: (a) $c_I = 3\times10^{-5}$; (b) $c_I = 3\times10^{-3}$.

IV. CONCLUSIONS

Our analysis of the critical behavior of the gel fraction and the susceptibility strengthens the conclusions drawn by HLS: within the errors of the data, the critical exponents β, ν, and γ for kinetic gelation are indistinguishable from those for percolation but the critical amplitude ratio C^-/C^+ is not universal, opposing the conclusion of Aharony for percolation that this amplitude ratio is universal. Comparison with experiment is not very conclusive at this time; the most recent measurements[37] indeed show good agreement with the critical exponents of kinetic gelation and of three-dimensional percolation. The relatively low observed value of the amplitude ratio, $R \sim 1$, may result from the kinetics of the radical initiated growth, but here experimental results are too preliminary to be conclusive.[38] We also find that the gel point varies as $c_I^{1/3}$ as c_I changes by 4 orders of magnitude. A simple argument implies that this means that each walk which grows from an initiator has a fractal dimension of 2. This is the same exponent as found by Kremer and Lyklema for kinetic growth walks[8,9] (KGW) of "moderate" length. This might be a coincidence since our walks are not merely isolated KGW but hinder each other and might be subtly correlated. If, however, our walks really have the same properties as KGW, it is possible that for much smaller values of c_I the fractal dimensionality will cross over to a value of $\frac{5}{3}$. Our data for the backbone for $c_I = 3\times10^{-4}$ show a distinctly different value for the fractal dimension than that calculated for percolation. It seems, therefore, that the backbone exponent for kinetic gelation behaves independently of the bulk property exponents. Another difference between kinetic gelation and percolation is that the same cluster-size distribution scaling form which works quite beautifully for percolation does not seem to apply to our present results. We propose a new, generalized scaling form in which an oscillatory

function depending on a normalized variable s/s^* is explicitly introduced. We conclude, therefore, that kinetic gelation is apparently not in the same universality class as percolation. Furthermore, we see no clear evidence for crossover to a new universality class for $c_I \to 0$, although the possibility that such behavior could occur for very small values of c_I has been raised.[39]

ACKNOWLEDGMENTS

This research was supported in part by National Science Foundation Grant No. DMR-8300754. One of us (H.J.H.) also wishes to thank the Center for Simulational Physics at the University of Georgia for its hospitality during a portion of the time this work was carried out.

*Present address: Mason Laboratory, Yale University, New Haven, Connecticut 06520.

†Present address: Advanced Computational Methods Center, University of Georgia, Athens, Georgia 30602.

[1]P. J. Flory, J. Am. Chem. Soc. **63**, 3083 (1941); **63**, 3091 (1941); **63**, 3096 (1941).

[2]W. H. Stockmayer, J. Chem. Phys. **11**, 45 (1942); **12**, 125 (1944).

[3]P. G de Gennes, J. Phys. (Paris) Lett. **37**, L1 (1976).

[4]D. Stauffer, J. Chem. Soc. Faraday Trans. 2 **72**, 1354 (1976); Phys. Rev. Lett. **41**, 1333 (1978).

[5]H. J. Herrmann, D. P. Landau, and D. Stauffer, Phys. Rev. Lett. **49**, 412 (1982); H. J. Herrmann, D. Stauffer, and D. P. Landau, J. Phys. A **16**, 1221 (1983).

[6]P. Manneville and L. de Seze, *Numerical Methods in the Study of Critical Phenomena,* edited by I. Della Dora, J. Demongeot, and B. Lacolle (Springer, Berlin, 1981).

[7]For a general introduction to these growth processes see H. J. Herrmann, in *Kinetics of Aggregation and Gelation,* edited by F. Family and D. P. Landau (North-Holland, Amsterdam, 1984); see also H. J. Herrmann, Phys. Rep. **136**, 153 (1986).

[8]D. J. Amit, G. Parisi, and L. Peliti, Phys. Rev. B **27**, 1635 (1983).

[9]J. W. Lyklema and K. Kremer, in *Kinetics of Aggregation and Gelation,* edited by F. Family and D. P. Landau (North-Holland, Amsterdam, 1984); J. Phys. A **17**, L691 (1984).

[10]I. Majid, N. Jan, A. Coniglio, and H. E. Stanley, Phys. Rev. Lett. **52**, 1257 (1984). See also K. Kremer and J. W. Lyklema, *ibid.* **55**, 2091 (1985); I. Majid, N. Jan, A. Coniglio, and H. E. Stanley, *ibid.* **55**, 2092 (1985).

[11]T. A. Witten and L. Sander, Phys. Rev. Lett. **47**, 1400 (1981); P. Meakin, Phys. Rev. A **27**, 604 (1983).

[12]P. Meakin, Phys. Rev. Lett. **51**, 1119 (1983).

[13]M. Kolb, R. Botet, and R. Jullien, Phys. Rev. Lett. **51**, 1123 (1983).

[14]M. Kolb and H. J. Herrmann, J. Phys. A **18**, L435 (1985).

[15]T. Vicsek and F. Family, Phys. Rev. Lett. **52**, 1669 (1984).

[16]D. Matthews-Morgan, D. P. Landau, and H. J. Herrmann, Phys. Rev. B **29**, 6328 (1984).

[17]M. E. Fisher, in *Critical Phenomena,* edited by M. S. Green (Academic, New York, 1971), p. 1.

[18]A. Margolina and H. J. Herrmann, Phys. Lett. **104A**, 295 (1984).

[19]J. W. Essam and M. E. Fisher, J. Chem. Phys. **38**, 802 (1963). See also M. E. Fisher, Physics (N.Y.) **3**, 255 (1967), and references thererin.

[20]S. Kirkpatrick, *Electrical Transport and Optical Properties of Inhomogeneous Media (Ohio State University),* Proceedings of the Conference on the Electrical Transport and Optical Properties of Inhomogeneous Media, edited by J. C. Garland and D. B. Tanner (AIP, New York, 1978), p. 99.

[21]A. Skal and B. I. Shklovskii, Fiz. Tekh. Poluprovodn. **8**, 1586 (1974) [Sov. Phys.—Semicond. **8**, 1029 (1975)].

[22]Y. Kantor and I. Webman, Phys. Rev. Lett. **52**, 1891 (1984).

[23]R. Pike and H. E. Stanley, J. Phys. A **14**, L169 (1981); A. Coniglio, Phys. Rev. Lett. **46**, 250 (1981).

[24]L. de Arcangelis, S. Redner, and A. Coniglio, Phys. Rev. B **31**, 4725 (1985).

[25]H. J. Herrmann, D. C. Hong, and H. E. Stanley, J. Phys. A **17**, L261 (1984).

[26]D. W. Heermann and D. Stauffer, Z. Phys. B **44**, 339 (1981); A. Margolina, H. J. Herrmann, and D. Stauffer, Phys. Lett. **93A**, 73 (1982).

[27]A. Aharony, Phys. Rev. B **22**, 400 (1980).

[28]D. Stauffer, *Introduction to Percolation Theory* (Taylor and Francis, London, 1985).

[29]N. Jan, T. Lookman, and D. Stauffer, J. Phys. A **16**, L117 (1983); R. Bansil, B. Carvalho, and H. J. Herrmann, *ibid.* **18**, L159 (1985).

[30]A. Chhabra, D. Matthews-Morgan, D. P. Landau, and H. J. Herrmann, J. Phys. A **18**, L575 (1985).

[31]D. Matthews-Morgan and D. P. Landau, in *Kinetics of Aggregation and Gelation,* edited by F. Family and D. P. Landau (North-Holland, Amsterdam, 1984).

[32]E. Donoghue and J. H. Gibbs, J. Chem. Phys. **70**, 2346 (1979).

[33]L. Leibler and F. Schosseler, Phys. Rev. Lett. **55**, 1110 (1985).

[34]P. Grassberger, J. Phys. A **78**, L215 (1985); S. Havlin and R. Nossal, *ibid.* **17**, L427 (1984); R. Rammal, J. C. Angles d'Auriac, and A. Benoit, *ibid.* **17**, L491 (1984).

[35]A preliminary report on the backbone was presented by Ashvin Chhabra, H. J. Herrmann, and D. P. Landau, *Fractals in Physics,* edited by L. Pietranero and E. Tosatti (North-Holland, Amsterdam, 1986).

[36]H. J. Herrmann and H. E. Stanley, Phys. Rev. Lett. **53**, 1121 (1984).

[37]M. Adam (private communication).

[38]D. Stauffer, Physica **106A**, 177 (1981).

[39]N. Jan, A. Coniglio, H. J. Herrmann, D. P. Landau, F. Leyvraz, and H. E. Stanley, J. Phys. A **19**, L399 (1986).